

SLOW TEMPERATURE EQUILIBRATION BEHIND THE SHOCK FRONT OF SN 1006

JACCO VINK^{1,2}, J. MARTIN LAMING³, MING FENG GU^{2,4}, ANDREW RASMUSSEN¹, JELLE S. KAASTRA⁵
Draft version October 30, 2018

ABSTRACT

We report on the observation of O VII Doppler line broadening in a compact knot at the edge of SN 1006 detected with the Reflective Grating Spectrometer on board *XMM-Newton*. The observed line width of $\sigma = 3.4 \pm 0.5$ eV at a line energy of 574 eV indicates an oxygen temperature of $kT = 528 \pm 150$ keV. Combined with the observed electron temperature of ~ 1.5 keV the observed broadening is direct evidence for temperature non-equilibration in high Mach number shocks, and slow subsequent equilibration. The O VII line emission allows an accurate determination of the ionization state of the plasma, which is characterized by a relatively high forbidden line contribution, indicating $\log(n_e t) \simeq 9.2$.

Subject headings: shock waves – X-rays: observations individual (SN 1006) – supernova remnants

1. INTRODUCTION

It has been suspected for many years that the high Mach number, collisionless shocks of young supernova remnants (SNRs) do not produce electron-ion temperature equilibration. The Rankine-Hugoniot relations require that for very high Mach numbers the temperature for each particle species i :

$$kT_i = \frac{2(\gamma - 1)}{(\gamma + 1)^2} m_i v_s^2 = \frac{3}{16} m_i v_s^2, \quad (1)$$

with m_i the particle mass, v_s the shock velocity, and γ the ratio of specific heats, usually taken to be $5/3$ (e.g. McKee & Hollenbach 1980). The heating process in collisionless shocks is not well understood, but the Coulomb collision times are too long to provide the required heating. So other, collective, processes should be responsible for the heating. This raises the question whether the heating process leads to temperature equilibration or not, i.e. is the electron temperature very low compared to the proton temperature, which, according to (1), should be lower than the oxygen or iron temperature? If temperatures are not equilibrated at the shock front, and subsequent equilibration proceeds through Coulomb interactions, full equilibration takes $\sim 10^{12}/n_e$ s (see Itoh 1984).

A clear hint for non-equilibration is the low electron temperature in young SNRs, which in no object seem to exceed 5 keV, whereas a typical shock velocity of 4000 km/s should give rise to a mean plasma temperature of 19 keV (e.g. McKee & Hollenbach 1980; Hughes et al. 2000). X-ray observations usually allow only the electron temperature to be determined from the continuum shape and line ratios. The ion temperature is difficult to measure, as it does not alter the continuum shape, and hardly influences the ionization and excitation balance.

Some measurements of temperature non-equilibration based on optical and UV spectroscopy have been reported. The shock velocity and amount of electron-proton equilibration can be determined from the line widths and ratio of H α and H β emission from non-radiative shocks. For the northwestern shock front in SN 1006, which is also the subject of this letter, Ghavamian et al. (2002) measured a shock velocity from the H α width of $v_s = 2890$ km/s and inferred an electron to proton tempera-

ture ratio $T_e/T_p < 0.07$. Together with the measured proper motion Winkler et al. (2003) were able to determine a distance to SN 1006 of 2.17 ± 0.08 kpc. UV spectra obtained with the Hopkins Ultraviolet Telescope showed broad C IV, N V and O VI lines, indicating temperature non-equilibration of these elements (Raymond et al. 1995), and a comparison of these line intensities with He II allowed a measurement of $T_e/T_p < 0.05$ (Laming et al. 1996). X-ray observations of SN 1006 indicate a low value of typically $\log(n_e t) \sim 9.5$ (Vink et al. 2000; Dyer et al. 2001), implying that if the equilibration is governed by Coulomb interactions, the plasma did not have sufficient time to equilibrate.

Here we report on a direct X-ray measurement of the O VII temperature in the northwest of SN 1006. It confirms with a high statistical confidence the slow equilibration of electron and ion temperature, but for a position further downstream from the shock than for the optical and UV measurements.

2. OBSERVATIONS AND METHODS

We observed SN 1006 (G327.6+14.6) with the *XMM-Newton* X-ray observatory (Jansen et al. 2001) with the goal of measuring the ionization and equilibration in SN 1006. The two observations are part of the guest observer program and were made on August 10 and 11, 2001. One observation pointed on the bright knot in the northwest, the main topic of this letter, the other on the narrow filaments in the east of SN 1006. The exposure times varied per instrument, but were close to 60 ks for both observations. In order to produce Fig. 1 we also used additional archival *XMM-Newton* and *Chandra* data.

Our main result is obtained with the Reflective Grating Spectrometer (RGS, den Herder et al. 2001). The two RGS instruments, RGS1 and RGS2 cover the wavelength range of $\sim 6-40$ Å, with a first order resolution of $\lambda/\Delta\lambda \sim 300$ at 20 Å. Emissions from different orders are separated using the intrinsic energy resolution of the CCDs. Unfortunately one CCD chip on the RGS1 and one on the RGS2 no longer function. As a result the RGS1 spectrum does not cover the wavelength range encompassing Ne line emission, and the RGS2 does not

¹ Columbia Astrophysics Laboratory, Columbia University, MC 5247, 550 W 120th street, New York, NY 10027, USA; jvink@astro.columbia.edu

² Chandra fellow

³ Naval Research Laboratory, Code 7674L, Washington DC 20375, USA

⁴ Center for Space Research, MIT, Cambridge, MA 02139

⁵ SRON National Institute for Space Research, Sorbonnelaan 2, NL-3584 CA, Utrecht, The Netherlands

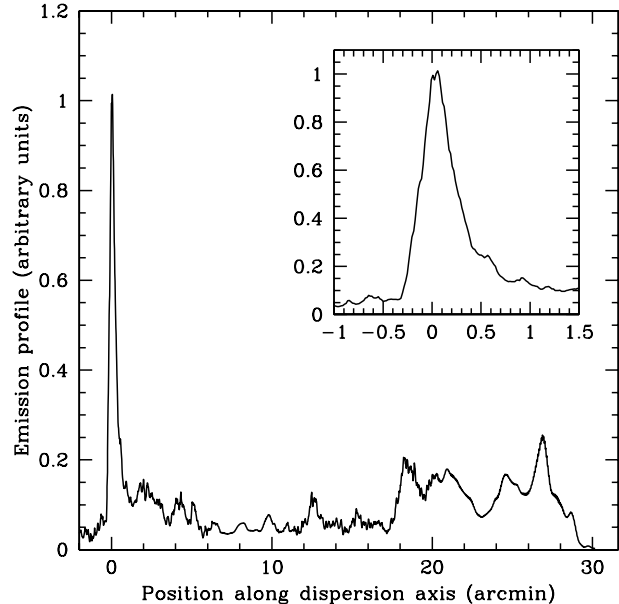
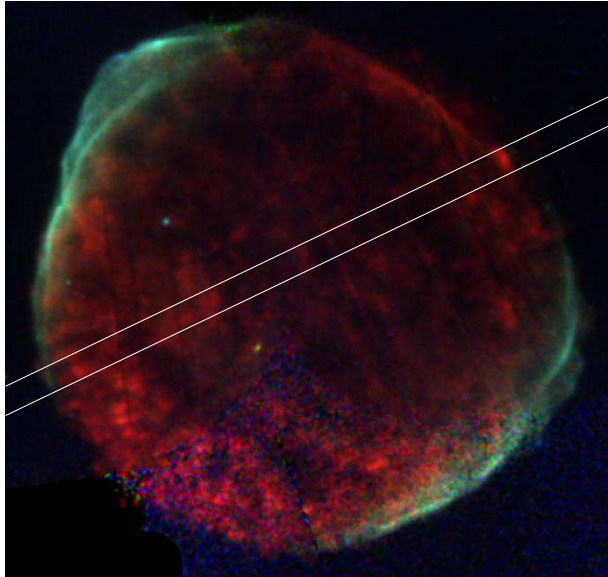


FIG. 1.— *Left*: *XMM-Newton* image of SN 1006 with the following color coding: red, 0.5-0.61 keV (dominated by O VII He α); green, 0.75 - 1.6 keV; blue, 1.6 - 7 keV. The area contributing to the RGS spectra is indicated by the two lines. *Right*: OVII emission profile along the dispersion direction of the RGS (based on a combination of EPIC and *Chandra* data). The inset shows the profile of the bright northwestern knot (*Chandra*).

cover the wavelength range around 22 Å, which contains the O VII He α line emission. We limited the extraction region to an 1' wide strip across the bright northwestern knot.

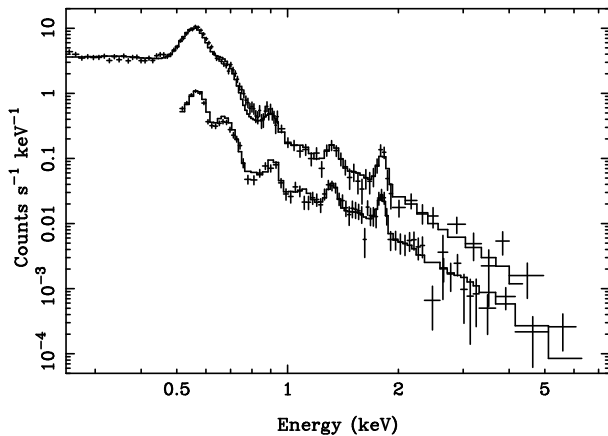


FIG. 2.— EPIC-CCD spectra of the bright knot in the northwest of SN 1006. The solid line is the best fit single NEI model (see Table 1). The top spectrum is the EPIC-PN (x5), the bottom spectrum is the combined EPIC-MOS spectrum.

The extended emission from SN 1006 means that the standard response matrices had to be convolved with the spatial emission profile displayed in Fig. 1, with an attenuation due to off-axis telescope vignetting. The bright knot has a spatial width of 0.4' (FWHM), which gives an apparent spectral broadening of $\Delta\lambda = 0.05$ Å (FWHM), or $\lambda/\Delta\lambda = 430$ at 21.6 Å. The intrinsic resolution of the RGS is $\Delta\lambda = 0.06$ Å (den Herder et al. 2001). As the knot is compact and close to the edge of SN 1006 it is unlikely that any measurable broadening is due to bulk motions along the line of sight.

XMM-Newton also has CCD cameras behind each of its three mirrors, called the European Photon Imaging Camera (EPIC). We use the spectra extracted from the EPIC data to measure

the electron temperature and abundances. All standard data reductions and response matrix calculations were done with SAS 5.3.3. Background spectra for the EPIC data were taken from a region outside SN 1006, but close to the center of the field. As RGS background spectra we used archival data of targets with no apparent line emission, such as gamma ray bursts.

3. THE ELECTRON AND ION TEMPERATURES IN THE NORTHWEST OF SN 1006

The measurement of the non-equilibration of the electron and ion temperatures requires the measurement of both the ion temperature, here oxygen temperature, and the electron temperature.

The electron temperature is in this case most accurately measured from the spectral continuum shaped observed with the EPIC CCD spectra, as the low ionization time scales in SN 1006 make the available line ratios only weakly temperature dependent. The EPIC spectra from the northwestern knot were fitted with the *SPEX* non-equilibration ionization (NEI) code (Kaastra et al. 1996). As the knot is relatively compact, temperature and ionization gradients are probably of minor importance. The plasma parameters obtained by fitting the spectra indicate $\log(n_e t) = 9.4$, and $kT_e \sim 1.3 - 1.7$ keV, higher than the $kT_e \sim 0.7$ keV reported by Long et al. (2003) based on *Chandra* data. Note, however, that the *Chandra* spectra have a lower spectral resolution, and have currently more calibration problems. Moreover, as there are two different kind of EPIC instruments, we were able to verify the consistency of the results (Fig. 2). Nevertheless, the measured kT_e is substantially lower than the $kT_e \sim 20$ keV expected for a fully equilibrated plasma, but still higher than that expected from Coulomb equilibration alone behind a 3000 km/s shock. Fig. 3 shows the predicted kT_e against $n_e t$ for current observations of the SN 1006 knot, as well as the various ion temperatures. Our fitted $n_e t$ corresponds to plasma shocked 200-300 years ago, which is predicted to

have $kT_e = 600$ eV. Hence we infer a small degree of collisionless electron heating (around 5% of the shock energy, i.e. $T_e/T_p \sim 0.1$, see Ghavamian et al. (2001)) consistent with optical and UV observations (Ghavamian et al. 2002; Laming et al. 1996) of SN 1006 and with observations of high Mach number shocks in other supernova remnants such as Tycho (Ghavamian et al. 2001) and SN 1987A (Michael et al. 2002).

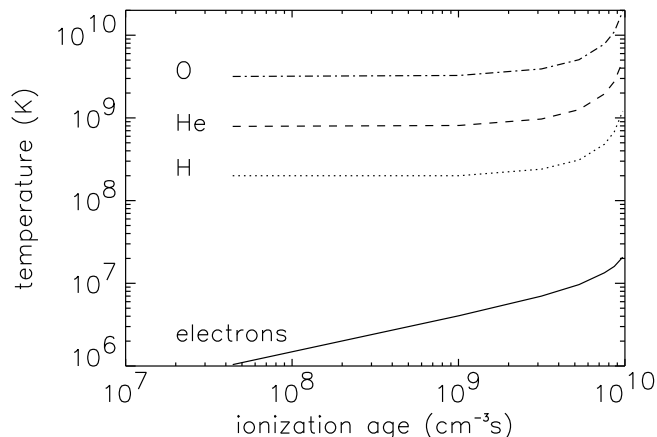


FIG. 3.— Expected relation between $n_e t$ and electron and ion temperature based on a shock history model for the SN 1006 blast wave (Truelove & McKee 1999; Laming 2001).

The spectra are dominated by line emission from O VII, the other line complexes are, however, not from helium-like stages of Ne, Mg and Si, as identified by Long et al. (2003), but from lower ionization stages. For instance the EPIC spectra show consistently that the Mg line centroid is 1.33 ± 0.01 keV, whereas the Mg XI line centroid is 1.35 keV. The Si line centroid is 1.80 ± 0.01 keV, which differs significantly from the Si XIII centroid of 1.85 keV. Instead these centroids indicate ionization stages around Mg IX and Si IX. The Ne centroid, as determined from the RGS2 spectrum, indicates 0.900 ± 0.004 keV, consistent with Ne VII. These centroids provide clear evidence for extreme NEI conditions for the northwestern knot and corroborate the measured $n_e t$ value.

TABLE 1
BEST FIT NEI MODEL

Parameter	NW Bright knot
kT_e (keV)	1.5 ± 0.2
$n_e t$ ($10^9 \text{ cm}^{-3} \text{ s}^{-1}$)	2.35 ± 0.07
N	0.25 ± 0.09
O	0.48 ± 0.04
Ne	0.14 ± 0.02
Mg	0.56 ± 0.14
Si	2.6 ± 0.5
$n_H n_e V / 4\pi d^2$ (10^{11} cm^{-5})	1.9 ± 0.2
χ^2/ν	324/169

Note. — The absorption column density was fixed to $6.8 \times 10^{20} \text{ cm}^{-2}$ (Dubner et al. 2002). Abundances are given with respect to the cosmic abundances of Anders & Grevesse (1989); errors were calculated using $\Delta\chi^2 = 2.7$ (90% confidence).

In agreement with Long et al. (2003) we find that the knot emission indicates an overabundance of Si, but contrary to the *Chandra* data we do find O, Ne and Mg to be somewhat underabundant (Table 1). This may indicate that instead of shocked ISM the knot is actually ejecta or ISM mixed with

ejecta. This does not diminish the evidence for temperature non-equilibration, but it makes it harder to combine the results reported here with the $H\alpha$ shock velocity measurements.

The RGS1 spectrum (Fig. 4) shows that the emission around 0.66 keV is dominated by O VII He β emission (O VIII Ly α : O VII He β \simeq 1 : 1.6). Ne is detected in the RGS2 spectrum, but Mg and Si are too weak for the RGS instruments. No evidence for Fe XVII line emission is seen at 15.01 Å, 16.78 Å, 17.0 Å, or 17.10 Å, presumably because Fe has not yet reached the Fe XVII charge state. The O VII emission is well described by $n = i \rightarrow 1$, line ratios that scale with the ratios of the oscillator strengths, as is expected for $kT_e \gtrsim 1$ keV.

In order to measure the ion temperature through the thermal Doppler broadening we fitted the RGS1 spectrum in the range from 21.0 – 22.3 Å, dominated by oxygen line emission, with six absorbed gaussians and a bremsstrahlung continuum with $kT_e = 1.5$ keV fixed to the continuum outside the fitted range ($N_H = 6.8 \times 10^{20} \text{ cm}^{-2}$, Dubner et al. 2002). The six gaussian components had centroids fixed at the energies of the bright O V, O VI, and O VII lines. The ratios of those lines were fixed according to calculations with the FAC atomic code (Gu 2002), for $kT_e = 1.5$ keV and a grid of $n_e t$ values between $\log(n_e t) = 9.0 - 9.4$. The line broadening was taken to be proportional to the line energies. Spectral fitting was done with spectral fitting package *xspec* (Arnaud 1996). This allowed us to use the C-statistic, which is the maximum likelihood statistic appropriate for Poisson noise (Cash 1979).

The best fits corresponded to $\log(n_e t) = 9.18$ with a maximum likelihood statistic of $C = 93.6$ for 104 data bins, with a possible range of $\log(n_e t) = 9.04 - 9.30$. This is somewhat lower, but arguably more accurate, than the value derived from the CCD spectra. It is also consistent with the measured oxygen Ly α to He β ratio with the RGS. For higher value of $\log(n_e t)$ the emission would be much more dominated by the O VII resonance line at 21.6 Å, whereas the RGS1 spectrum indicates a substantial contribution of forbidden line emission at 22.1 Å due to O VI inner shell ionization and excitation.

The line broadening needed to obtain an acceptable fit is $\sigma_E = 3.4 \pm 0.5$ eV (68% confidence), if fitted within the wavelength range 21.4–22.6 Å. As Fig. 4 shows the broadening underpredicts the wing of the resonance line between 21.0–21.4 Å, which is a possible indication that the oxygen ions may not be completely thermalized (i.e. are not fully described by a Maxwellian distribution). The statistical confidence of the detection of line broadening is at the 9.8σ level ($\Delta C = 96.1$). The 99.73% (3σ) confidence range is 2.2 – 6.5 eV. Even if we do not fix the line ratios and optimize each individual line, we obtain $\sigma_E = 2.5 \pm 0.4$ eV with a statistical confidence still at the 6.5σ level. During our analysis we have compared different methods of analyzing the data, with various wavelength fitting ranges. This has given us some feeling of the systematic uncertainties involved. We estimate that the systematic error on σ_E is about 0.7 eV.

4. DISCUSSION

Our analysis of CCD and grating data of a bright knot in SN 1006 obtained by *XMM-Newton* shows that $kT_e \sim 1.5$ keV and $\log(n_e t) = 9.04 - 9.30$. The Doppler broadening at 574 eV is $\sigma_E = 3.4 \pm 0.5$ eV, which corresponds to an oxygen temperature of $kT_{oxygen} = 530 \pm 150$ keV (e.g. eq. 10.69 Rybicki & Lightman 1979). This indicates a shock velocity of > 4000 km/s, if no significant temperature equilibration has

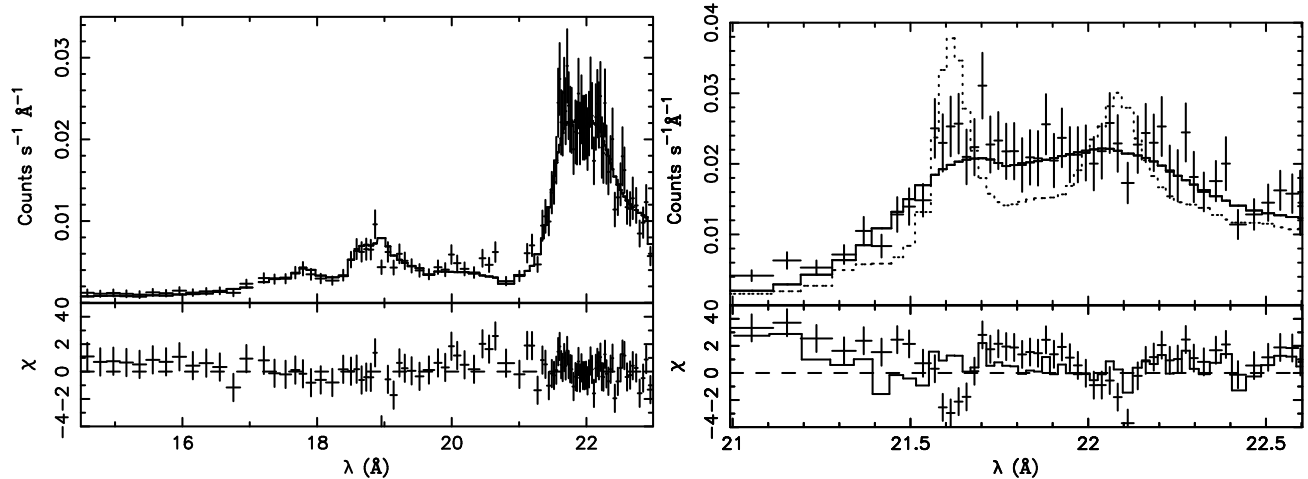


FIG. 4.— On the left: RGS1 spectrum showing O VII and O VIII line emission with line emission modelled by broadened gaussian shaped lines. On the right: The O VII triplet. The solid line indicate the best fit model with thermal Doppler broadening. The dotted line shows the best fit model without broadening. The residuals are shown as a connected line and crosses respectively.

taken place, but allowing for the possibility of some adiabatic cooling (eq. 1). The implied shock velocity is higher than the ~ 3000 km/s indicated by recent $H\alpha$ measurements (Ghavamian et al. 2002), but given the systematic errors both measurements agree.

The excess emission in the wings of the O VII line emission, although possibly due to calibration uncertainties concerning the wings of the intrinsic RGS line profiles, may also be real and caused by a lack of complete oxygen thermalization. This is not unexpected as the oxygen self equilibration time at high temperatures is comparable to the oxygen-proton equilibration time.

To conclude, the measured high oxygen ion temperature is a clear indication that the shock heating processes resulted in only a small degree (5%) of electron-ion equilibration at the shock front, and that the subsequent equilibration process is slow. This also has some bearing on the acceleration of cosmic rays in high Mach number shocks, which are thought to be injected into the shock acceleration process from the pool of the thermal gas behind the shock front. A low electron-ion equilibration will make it relatively more difficult for electrons

than for ions to be accelerated. However, the southwestern and northeastern limbs of SN 1006 are a prime examples of efficient electron acceleration as the X-ray emission from these parts is dominated by synchrotron emission (Koyama et al. 1995). Although we could not directly measure the electron temperature at those sites, the electron temperature close to the northwestern limb seems to be similar to that of northeastern knot. However, the notion of a thermal pool from which particles are accelerated is likely to be too simple, as recent simulations seem to indicate (Schmitz et al. 2002).

We thank John Peterson for making to us available his Monte Carlo Code which helped us verify the validity of our results. JV and MFG were supported for this work by the NASA through Chandra Postdoctoral Fellowship Award Number PF0-10011 & PF0-10014 issued by the Chandra X-ray Observatory Center, which is operated by the Smithsonian Astrophysical Observatory for NASA under contract NAS8-39073. JML was supported by the NASA Contract S 92540F from the XMM GI Program and by basic research funds of the Office of Naval Research.

REFERENCES

- Anders, E. & Grevesse, N. 1989, *Geochim. Cosmochim. Acta*, 53, 197
 Arnaud, K. A. 1996, in *ASP Conf. Ser. 101: Astronomical Data Analysis Software and Systems V*, Vol. 5, 17
 Cash, W. 1979, *ApJ*, 228, 939
 den Herder, J. W. et al. 2001, *A&A*, 365, L7
 Dubner, G. M., Giacani, E. B., Goss, W. M., Green, A. J., & Nyman, L.-Å. 2002, *A&A*, 387, 1047
 Dyer, K. K., Reynolds, S. P., Borkowski, K. J., Allen, G. E., & Petre, R. 2001, *ApJ*, 551, 439
 Ghavamian, P., Raymond, J., Smith, R. C., & Hartigan, P. 2001, *ApJ*, 547, 995
 Ghavamian, P., Winkler, P. F., Raymond, J. C., & Long, K. S. 2002, *ApJ*, 572, 888
 Gu, M. F. 2002, *ApJ*, 579, L103
 Hughes, J. P., Rakowski, C. E., & Decourchelle, A. 2000, *ApJ*, 543, L61
 Itoh, H. 1984, *ApJ*, 285, 601
 Jansen, F. et al. 2001, *A&A*, 365, L1
 Kaastra, J. S., Mewe, R., & Nieuwenhuijzen, H. 1996, in *Proc. of the 11th Coll. on UV and X-ray, UV and X-ray Spectroscopy of Astrophysical and Laboratory Plasmas*, ed. K. Yamashita & T. Watanabe (Tokyo:Universal Academy Press), 411
 Koyama, K., Petre, R., Gotthelf, E. V., Hwang, U., Matsuura, M., Ozaki, M., & Holt, S. S. 1995, *Nature*, 378, 255
 Laming, J. M. 2001, *ApJ*, 563, 828
 Laming, J. M., Raymond, J. C., McLaughlin, B. M., & Blair, W. P. 1996, *ApJ*, 472, 267
 Long, K. S., Reynolds, S. P., Raymond, J. C., Winkler, P. F., Dyer, K. K., & Petre, R. 2003, *ApJ*, in press
 McKee, C. F. & Hollenbach, D. J. 1980, *ARA&A*, 18, 219
 Michael, E., Zhekov, S., McCray, R., Hwang, U., Burrows, D. N., Park, S., Garmire, G. P., Holt, S. S., & Hasinger, G. 2002, *ApJ*, 574, 166
 Raymond, J. C., Blair, W. P., & Long, K. S. 1995, *ApJ*, 454, L31
 Rybicki, G. B. & Lightman, A. P. 1979, *Radiative processes in astrophysics* (New York, Wiley-Interscience, 1979. 393 p.)
 Schmitz, H., Chapman, S. C., & Dendy, R. O. 2002, *ApJ*, 570, 637
 Truelove, J. K. & McKee, C. F. 1999, *ApJS*, 120, 299
 Vink, J., Kaastra, J. S., Bleeker, J. A. M., & Preite-Martinez, A. 2000, *A&A*, 354, 931
 Winkler, P. F., Gupta, G., & Long, K. S. 2003, *ApJ*, submitted, (astro/0208415)